



Spatio-temporal trends in daily maximum rainfall in northwestern Algeria (Macta watershed case, Algeria)

Benali Benzater¹ · Abdelkader Elouissi² · Boumedienne Benaricha³ · Mohammed Habi⁴

Received: 9 January 2019 / Accepted: 17 April 2019 / Published online: 1 June 2019
© Saudi Society for Geosciences 2019

Abstract

Results of extreme precipitation trend analysis, at different spatial and temporal scales, have become alarming since the last century, due to the global climate change. This work describes the impact of climate change on the distribution and trend of maximum daily rainfall in the Macta watershed. Monthly maximum rainfall data that were collected over 41 years (1970 to 2010) on 41 stations were used to validate the present research. The extreme values of rainfall maxima (200 to 264 mm/d) are located in the northeastern part of the basin during the spring season. From 1992 onwards, shifts are observed from monthly, seasonal in addition to significant annual trends. Monthly, seasonal, and annual rainfall maxima trend analyses were identified using three methods, which are Mayer's adjustment method, Şen's innovative method (2012), and the Bravais-Pearson test. The study found out a downward trend during the first period (1970–1992). On the other hand, the second period (1992–2010) revealed significant upward trends. Climate change affects all regions except the center part of the study basin.

Keywords Algeria · Breaking · Climate change · Extreme rainfall · Macta trend

Introduction

The warming of the global climate system is unequivocal (IPCC 2007, 2013). Today, the questions, such as “Does the climate change?” “Will the earth warm up?”, no longer arise. Changes in weather and climate extremes impact and pose serious challenges for societies (CCSP 2008).

The analysis of extreme weather events related to climate change is one of the biggest challenges facing the scientific community because they have a major impact on the physical environment and the socio-economic sector (Kostopoulou and Jones 2005). Water resources, agriculture, ecosystems, forestry, health, insurance, and industry are some of the most

studied sectors (Parry et al. 2004). The extreme climate associated with temperature and precipitation can also affect energy consumption, human comfort, and tourism (Henderson and Muller 1997; Weisse 1998; Subak et al. 2000).

Several studies have been done on extreme rainfall trends (Caloieroa et al. 2016; Carvalho et al. 2014; Keggenhoff et al. 2014; Westra et al. 2012; Brugnara et al. 2012; Lopez-Moreno et al. 2011; Shang et al. 2011). There is substantial empirical and climatological evidence that extremes of precipitation increased during the twentieth century and that this trend is expected to continue with global warming (Mannshardt-Shamseldin et al. 2010).

Handling Editor: Fernando Al Pacheco

✉ Benali Benzater
benzaterbenali@univ-mascara.dz

Abdelkader Elouissi
elaek@yahoo.fr

Boumedienne Benaricha
benarichab@yahoo.fr

Mohammed Habi
moha.habi@gmx.de

¹ Biological Systems and Geomatics Research Laboratory (LRSBG), Faculty of Natural and Life Sciences, Mustapha Stambouli University of Mascara, Mascara, Algeria

² Biological Systems and Geomatics Research Laboratory (LRSBG), Faculty of Natural and Life Sciences, Mustapha Stambouli University of Mascara, Mascara, Algeria

³ Biological Systems and Geomatics Research Laboratory (LRSBG), Faculty of Natural and Life Sciences, Mustapha Stambouli University of Mascara, Mascara, Algeria

⁴ Faculté de technologie, Département d'hydraulique, University Abou Bakr Belkaid of Tlemcen, B.P. 119 13000 Tlemcen, Algeria

Understanding the spatial and temporal variability of extreme precipitation plays an important role in the management of water resources, particularly in flood mitigation and prevention. Knowledge of the distribution of spatio-temporal trends in extreme precipitation is crucial for hydrological flood control models using retention pond systems (Bellu et al. 2016) or surface water storage using rainwater harvesting systems (Terêncio et al. 2018; Terêncio et al. 2017). Sustainable protection-utilization plans must be implemented to ensure the sustainability of natural, historical, tourism, and cultural resources (Cetin et al. 2018a, b).

Recent years have seen a change in the rainfall pattern of daily rainfall in terms of frequency and intensity in some parts of the world. The findings of Min et al. (2011) and Westra et al. (2012) on extreme rainfall showed that nearly two-thirds of global rainfall stations have increasing trends. For instance, trends in annual maximum precipitation have increased in three regions studied in Brazil (Carvalho et al. 2014). Groisman et al. (2005), Sharad and Kumar (2012), and Sharad et al. (2017) have shown that the change observed in the rainfalls' intense frequency evolution in the world is greater than that observed in annual totals. Studies on extreme rainfall in the Mediterranean basin do not all converge towards the same results. Kioutsioukis et al. (2010) analyzed the extreme rains in Greece over the period (1955–2002) and found a decrease in their intensities. Alpert et al. (2002) showed an increase in extreme daily rainfall in Italy, Spain, and Cyprus during the period (1951–1995) associated with a decrease in total annual rainfall. Martinez et al. (2007) analyzed the variability of daily rainfall in the Catalan region of north-eastern Spain over the period (1950–2000) and showed a downward trend in daily extreme rainfall number.

The analysis of the Gorakhpur resort in India with a long data series reported the highest 24-h precipitation (2001 to June 2013) with an alarming increase in intensity. These events can be associated with regional warming and signal of the climate change effects on the region (Pandey 2014). Keggenhoff et al. (2014) showed slightly increasing trends in extreme daily rainfall in Georgia during the period 1971–2010. For monthly rainfall, there was a decreasing trend in the Per River Basin in China (Deng et al. 2018) and in Mediterranean areas (Elouissi et al. 2016; Longobardi and Villani 2009).

Seasonal accumulations of intense precipitation have decreased significantly in north-central Algeria, northern Italy, parts of southern France and Spain, and northern Portugal. Some of these observations are reported in several works (Alpert et al. 2002; Klein Tank and Können 2003; Brunetti et al. 2005; Kostopoulou and Jones 2005; Lopez-Moreno et al. 2011). Donat et al. (2014) indicated a different result, i.e., a significant increase in intense cumulative precipitation over northern Algeria. Trambly et al. (2013) suggested no significant trend in seasonal accumulations of rainfalls intense in northern Morocco or more widely throughout the Maghreb.

Shang et al. (2011) did not find a significant trend in the extreme rainfall records in northwestern Ethiopia.

During the 1990–1999 decade, which experienced a decrease in annual rainfall, floods became natural disasters resulting in numerous human casualties and extensive material damage in 1996 and 1998 in particular (Goula et al. 2007).

Like many continents in the world, Africa is experiencing the ravages of climate change, the mastery, and risk assessment of which depend in part on the knowledge and understanding of daily extreme rainfall (Ague and Afouda 2015).

Algeria, a Mediterranean country mostly located in semi-arid and arid zones, has always been confronted with droughts and extreme floods (Bekoussa et al. 2008; Meddi and Hubert 2003; Meddi et al. 2009), which constitute a real challenge to economic and social development. Algeria is among the countries at high climate change risk. It is ranked at as 59, with a World Risk Index (WRI) of 7.76% (United Nations University 2017). The WRI index is calculated based on natural factors, such as earthquakes, floods, and drought, on the country's susceptibility to disaster, coping skills, and the strategy of adaptation.

In this context of divergent results of the works cited above, on the one hand, and the impact of climate change and meteorological hazard on the other hand, this study analyzes the maximum daily, seasonal, and annual precipitation (MDP) in the North West of Algeria. One objective of this paper is to map the monthly, seasonal, and annual maximum daily rainfall collected on 41 stations during the period 1970–2010 in the Macta watershed (North-West Algeria). Another objective is the study of rainfall maxima series in order to identify the trends.

Study area

The study area is located in the Macta watershed, northwestern Algeria. Its geographical position is between -1.25° west and 0.60° east in longitude and between 34° and 36° north in latitude. The Macta is a basin that covers an area of $14,410 \text{ km}^2$. It is limited in the north-west by the mountain ranges of Tessala, in the south by the highlands of Maalif, in the west by the plateaus of Telagh and in the east by the Saida Mountains (Djediai 1997). The Macta basin is bordered in the north by the Mediterranean Sea, to the south by the mountains of Saida (1201 m) and Daya Mountains (1356 m), and to the southwest by the mountains of Tlemcen, including the mountains of Beni Chougrane and the plain of Mohamadia (Meddi and Toumi 2013). The average annual rainfall is rather low, which varies from 206 mm on the southern part of the Beni Chougrane Mountains (Bouhniaf and Sfisef) to 380 mm on Saïda Mountains and the northwestern part of Sidi Bel Abbas and Tessala Mountains (Elouissi et al. 2017). However, the spatial variation of average rainfall is moderate (25%). The Macta watershed is drained by two major rivers, which are

El-Hammam Wadi in the east and Wadi Mekker (called Wadi Mebtouh downstream), in the west (Fig. 1).

Data and methods

Data

The daily maximum precipitation data (DMP) (in mm) were collected by the National Office of Meteorology at Oran (ONM) and the National Agency for Water Resources (ANRH). Stations with high gap rates were discarded; only the stations with a gap rate not exceeding 10% were selected (Meddi and Assani 2014). Thus, 41 stations that have been selected are spread over all regions of the Macta watershed (Fig. 2). The observation period of these time series is 41 years (1970–2010). The selected rainfall stations are symbolized numerically (for example, Ras El Ma: 110102, Mascara: 111429).

Control and homogeneity of the data

Standard methods for the detection of point or systematic anomalies in data series (in particular, the analysis of cumulative regression residues between a reference variable deemed reliable and the variable to be tested) cannot be applied here because of the extreme nature of the rainfall variables (monthly daily maxima). Nevertheless, the graphical adjustment of the maximum annual rainfall to a statistic distribution of extreme events can at least visually prejudge the reliability of the data by the erroneous values (Berolo and Laborde 2003).

Adjustment of daily maximum precipitation to a probability distribution

The Gumbel distribution has long been the most used model for estimating quintiles. Koutsoyiannis (2004) showed that the

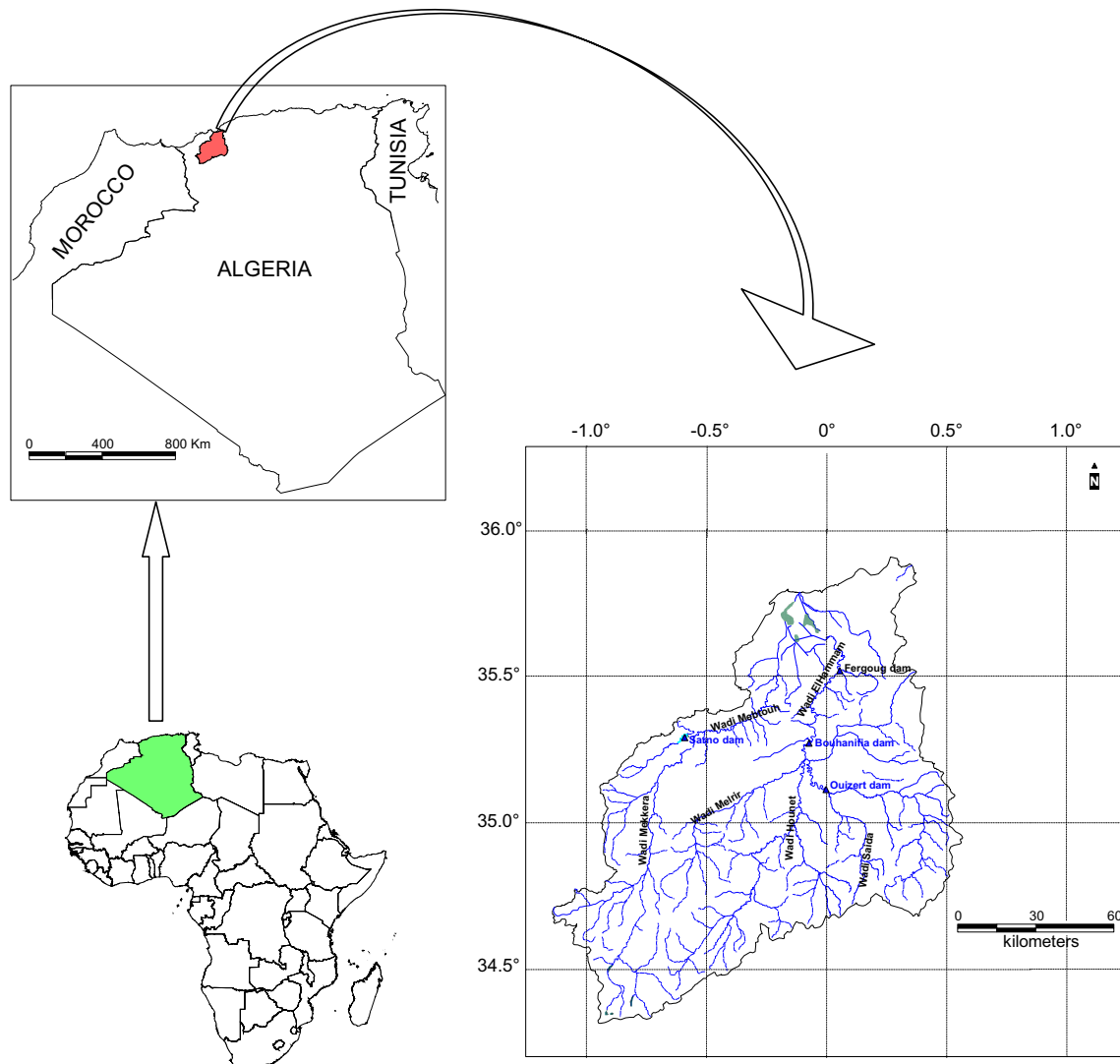


Fig. 1 Macta watershed situation

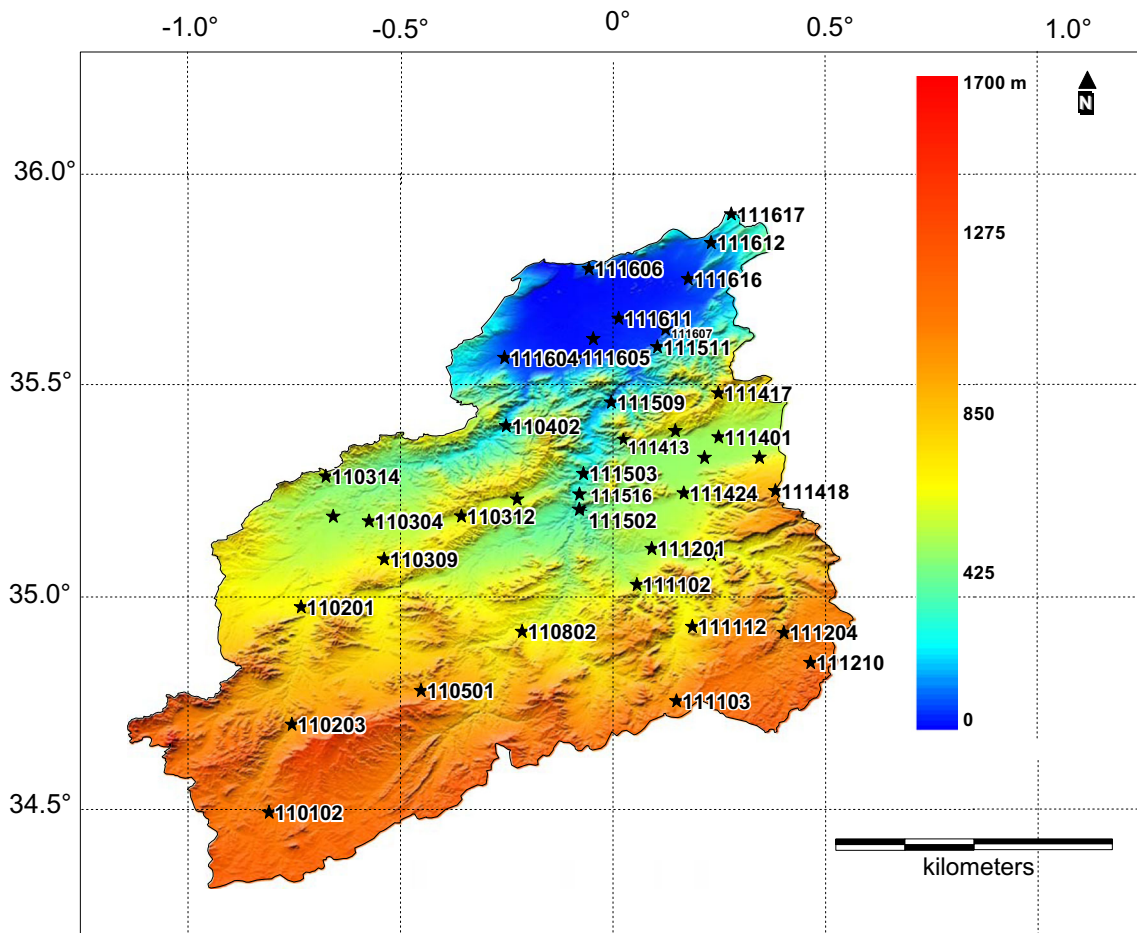


Fig. 2 Topographic map showing the location of the selected rainfall stations

application of Gumbel’s law can lead to a poor estimate of risk by underestimating the greatest extreme values of rainfall, especially when the series have a few decades of data and cannot have the same distribution as the actual one. Thus, many researchers prefer the generalized extreme values (GEV) law to Gumbel’s law for modeling maximum annual rainfall (Wilks and Cember 1993; Chaouche et al. 2002; Koutsoyiannis 2004; Onibon et al. 2004). The difference between quantiles estimated by the Gumbel law and the quantiles by the GEV law is considerable and can be two to three times larger (Muller 2006).

The extreme value theory has been used for the development of methods describing the behavior of extreme values, that is to say the points farthest from the mean. The widespread distribution of the extreme value-GEV shows great descriptive and predictive abilities to capture the asymmetry and kurtosis common to the data, without any prior constraints. It is robust in estimating quantiles of distribution and makes predictions on the return level (Mannshardt-Shamseldin et al. 2010; Zalina et al. 2002; Alentorn and Markose 2005).

The distribution function of the Jenkinson (1955) GEV law is expressed by Eq. (1):

$$F(x) = \exp \left\{ - \left[1 - \xi \frac{(x - \mu)}{\sigma} \right]^{1/\xi} \right\} \tag{1}$$

where $\mu, \sigma > 0$, and ξ are the location, scale, and shape parameters, respectively.

Figure 3 shows an example of extreme rainfall adjustment to the GEV law.

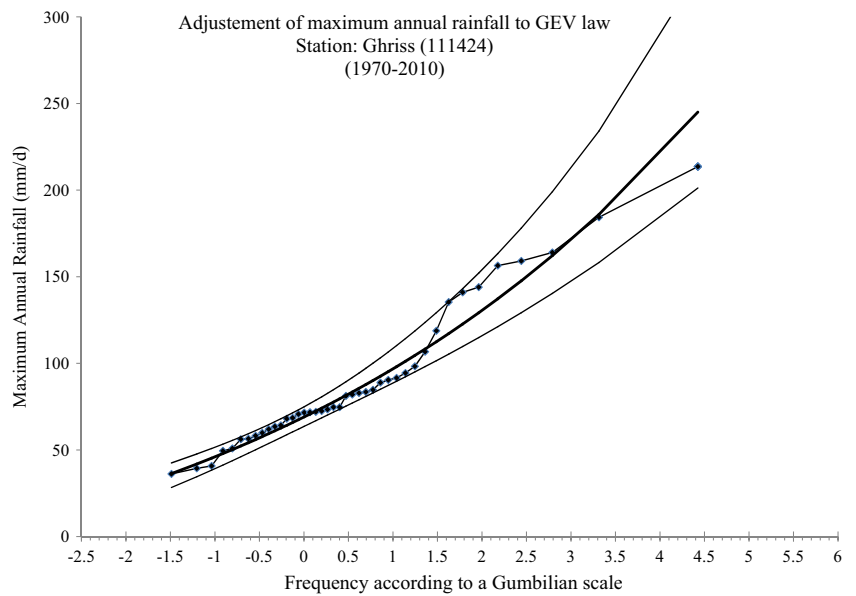
Description of the data

After detecting outliers (anomalies) and filling gaps, Fig. 4 shows the evolution of the annual extreme precipitation of the 41 stations of the Macta watershed during the period (1970–2010).

The statistical parameters of maximum annual rainfall are shown in Table 1.

According to Table 1, the maximum daily extreme rainfall values vary between 118.3 mm/day (Ras El Ma station: 110102) located south of the basin and 263.7 mm/day (Nesmoth MF station: 111418) located at East of the basin.

Fig. 3 Example of daily maximum rainfall adjustment to the GEV law



The variability of extreme rainfall is important. It is minimum (maximum) that appears at the Matemore (Trois Rivières) station with station number 111405 (111516) with a coefficient of variation of 27% (48%). The variation in the standard deviation varies between 21.5 (Matemore: 111405) and 50.8 (Nesmoth MF: 111418).

The analysis of Fig. 4 shows that the majority of the 41 stations converge to minimum values closer to the medians of the series. So, there is a dispersion of the annual maxima values at the beginning and the end of the time series, hence, the possible existence of a breaking in these series. The detection of a break in the series makes it possible to highlight the evolution of the rainfall regime

in the study region (Meddi et al. 2009). The minimum value of the cumulated maximum rainfall of the 41 stations corresponds to the year 1992, the probable date of climate change. Blanchet et al. (2018) identified this approximation of values for annual rainfall maxima between 1980 and 1990 in southern France, with 1985 as the most likely.

The innovative method of Şen (2012) and Mayer's is to split the time series into two equal periods, but as we suspect the existence of a break in these series, we then cut these series into two unequal periods following this suspicious year (1992): period I (1970–1992) with $n = 23$ years and period II (1992–2010) with $n = 19$ years.

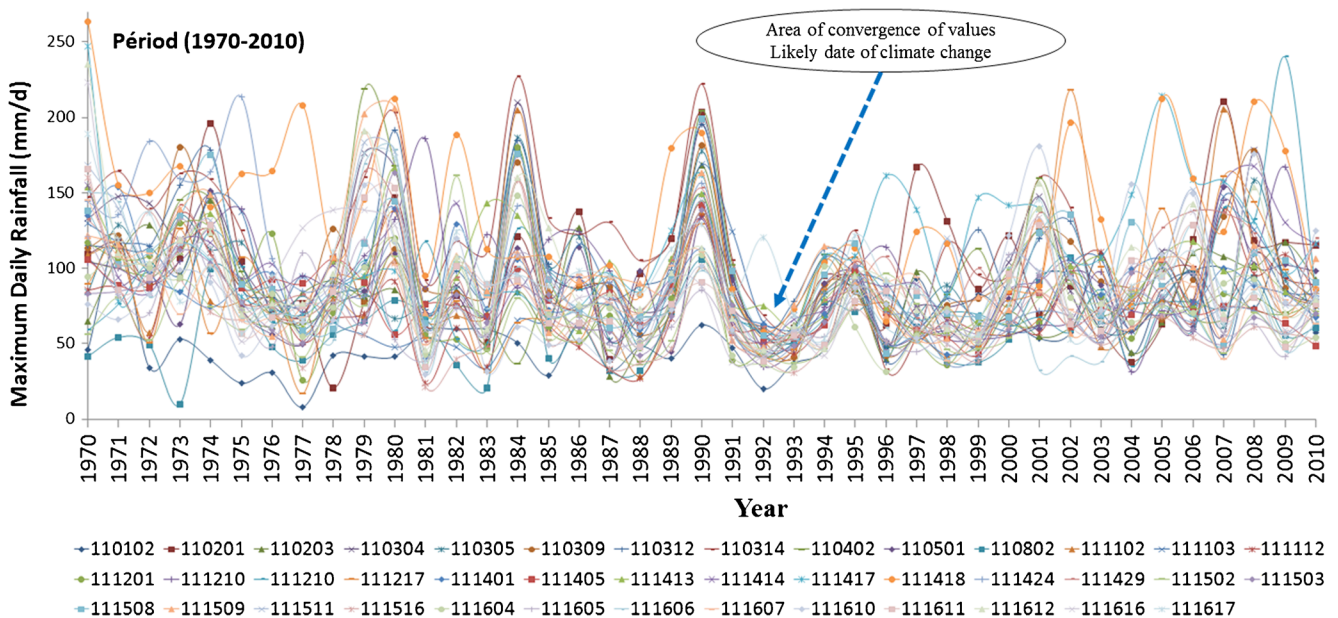


Fig. 4 Maximum annual rainfall for the 41 rainfall stations in the Macta watershed

Table 1 Statistical parameters of the annual maximum daily rainfall series of the 41 stations (period: 1970–2010)

Number	Station name	Station code	Longitude (°)	Latitude (°)	Z (m)	DMP (mm/day)	Average (mm/day)	Standard deviation	Coefficient of variation CV (%)
1	RAS EL MA	110,102	-0,809,334	34,494,740	1097	118,3	57,8	26,7	46
2	SID ALI BEN YOUB	110,201	-0,734,043	34,978,248	635	210,7	99,1	43,1	44
3	EL HACAIBA	110,203	-0,755,568	34,702,013	950	168,0	80,8	29,7	37
4	SARNO Bge	110,304	-0,574,060	35,180,350	425	209,7	101,2	41,2	41
5	SIDI BEL ABBES	110,305	-0,658,583	35,191,520	485	186,4	88,6	32,1	36
6	HASSI DAHO	110,309	-0,538,585	35,091110	650	181,6	95,3	35,2	37
7	MOSTEFA BEN BRAHIM	110,312	-0,356,967	35,192,004	590	195,3	99,9	37,1	37
8	AIN TRID	110,314	-0,675,747	35,285,762	530	226,8	115,0	43,8	38
9	CHEURFAS BGE	110,402	-0,251,628	35,404,398	230	218,9	90,3	41,1	46
10	MERINE	110,501	-0,451,765	34,781,331	970	153,8	81,3	28,5	35
11	DAOUD YOUB	110,802	-0,214,122	34,920,480	660	178,7	64,7	28,9	45
12	MEFTAH SIDI BOUBEKEUR	111,102	0,055986	35,031000	530	205,2	81,5	37,0	45
13	AIN EL HADJAR	111,103	0,149,130	34,757,058	1025	168,8	88,7	31,9	36
14	HAMMAM RABI	111,112	0,186,280	34,931,920	710	138,8	74,7	28,4	38
15	OUED TARIA	111,201	0,091058	35,115,659	501	180,1	79,3	32,4	41
16	AIN TIFRIT	111,204	0,401,859	34,917,816	970	185,7	93,5	35,3	38
17	TAMESNA	111,210	0,464,584	34,847,322	1105	239,9	84,9	37,2	44
18	BENIANE	111,217	0,231,450	35,101,077	630	218,3	86,2	38,4	45
19	MAOUSSA	111,401	0,248,202	35,378,314	494	153,5	85,6	26,3	31
20	MATEMORE	111,405	0,215,025	35,329,824	482	142,0	79,1	21,5	27
21	TIZI	111,413	0,076127	35,320,075	453	166,4	96,6	27,7	29
22	SIDI KADA	111,414	0,344,322	35,330,201	549	167,3	93,5	29,7	32
23	AIN FARES	111,417	0,247,782	35,481,576	806	247,0	110,9	40,8	37
24	NESMOTH MF	111,418	0,381,819	35,251,571	930	263,7	133,5	50,8	38
25	GHRIS	111,424	0,166,501	35,246,272	498	213,6	90,2	41,1	46
26	MASCARA	111,429	0,146,428	35,392,860	550	164,1	96,5	32,6	34
27	SAHOUE OUIZERT	111,502	-0,079531	35,207,846	361	161,0	66,7	24,3	36
28	BOU HANIFIA BGE	111,503	-0,069807	35,291,959	306	174,9	75,5	29,8	39
29	SFISSEF	111,508	-0,226,020	35,231,837	545	199,1	96,4	36,1	37
30	HACINE	111,509	-0,004537	35,459,880	145	206,0	95,4	37,5	39
31	MOHAMMADIA GRHA	111,511	0,104,206	35,590,378	50	183,1	93,6	34,5	37
32	TROIS RIVIERES	111,516	-0,085948	35,218,519	315	159,8	65,5	31,2	48
33	OGGAZ	111,604	-0,255,370	35,564,871	73	148,0	78,0	27,9	36
34	BOU HENNI	111,605	-0,086492	35,565,329	26	132,5	72,8	24,5	34
35	FORNEKA	111,606	-0,056751	35,774,381	78	178,2	79,4	35,6	45
36	SAMOURIA	111,607	0,115,319	35,622,188	48	189,6	82,2	28,2	34
37	MOCTA DOUZ	111,610	-0,046623	35,609,550	18	180,6	83,4	38,8	47
38	FERME BLANCHE	111,611	0,013060	35,657,361	20	165,6	83,4	31,0	37
39	BLED TAOURIA	111,612	0,230,748	35,835,681	118	234,9	96,9	40,3	42
40	MARAIS DE SIRAT	111,616	0,176,414	35,750,668	30	223,0	87,0	36,6	42
41	FERME ASSORAIN	111,617	0,277,981	35,902,936	222	189,0	95,5	34,5	36

Study of maximum daily precipitation trends

Nowadays, the effects of global climate change have been remarkably perceived, and thus, the determination of precipitation trends has become crucial for water source planning and the engineering phases of future projects.

Several methods are used for trend detection including Bravais-Pearson r , Spearman rho (SMR), Mann-Kendall tau (MK), Sen method (1968), innovative method of Şen (2012), and the test of cumulative rank difference (CRD) (Onyutha 2015).

The analysis adopted in this article is inspired by three methods: Mayer's adjustment method, Şen's innovative method (Şen 2012), and the Pearson-Bravais test. It consists of the following steps:

1. Cut the time series of daily maximum precipitation (monthly, seasonal, and annual) in two (02) periods: period I and period II.
2. Correlate daily rainfall maxima over time (years) for both periods I and II.
3. For each period, estimate extreme rainfall trends by calculating the Bravais-Pearson correlation coefficient

Table 2 Westmacott trend classifications

Category	Strong increasing trend SIT	Moderate increasing trend MIT	Non-significant trend NST	Moderate decreasing trend MDT	Strong decreasing trend SDT
r	$r > 0$ and $\alpha \leq 0.05$	$r > 0$ and $0.05 < \alpha \leq 0.10$	$\alpha > 0.10$	$r < 0$ and $0.05 < \alpha \leq 0.10$	$r < 0$ and $\alpha \leq 0.05$

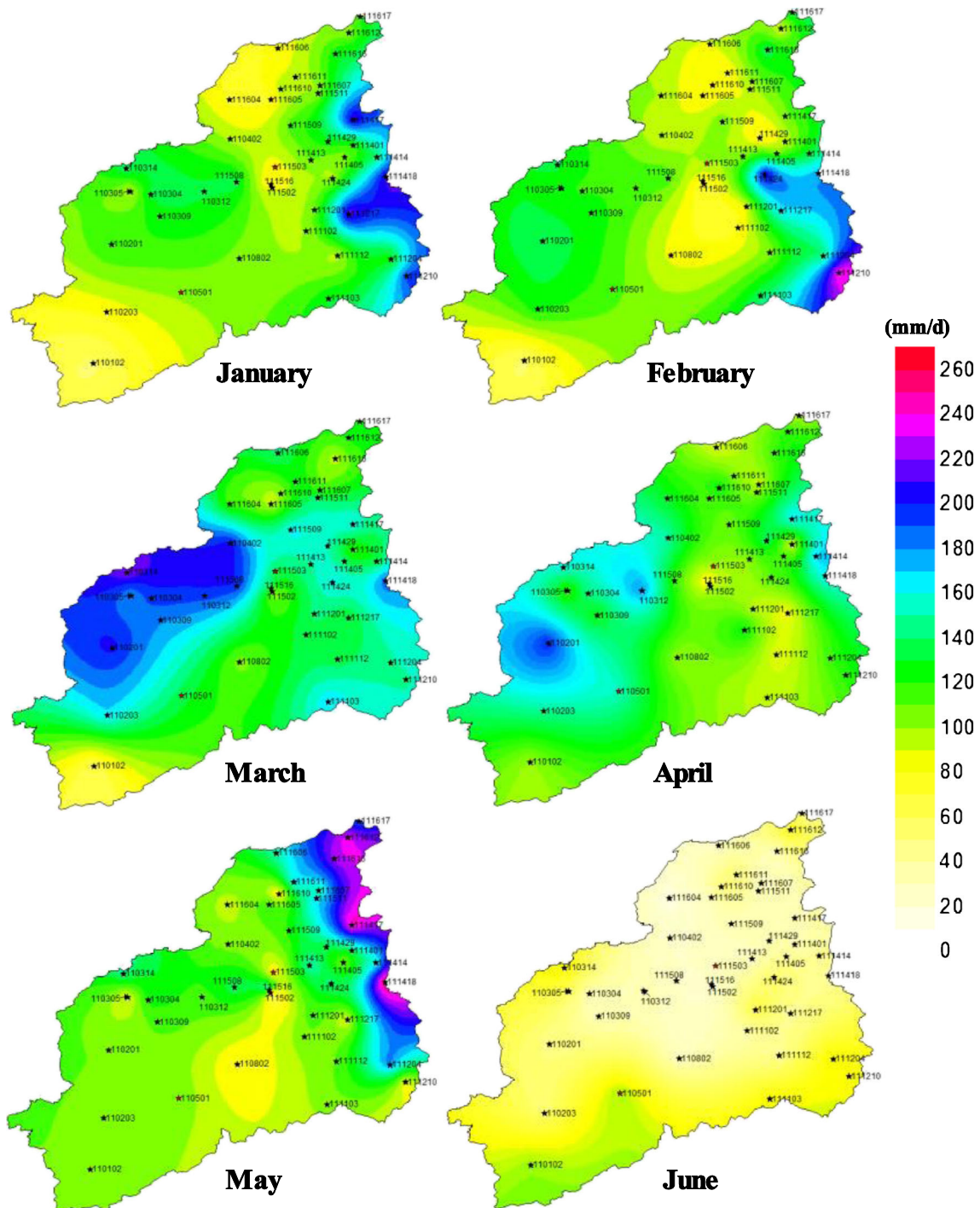


Fig. 5 Maximum monthly rainfall

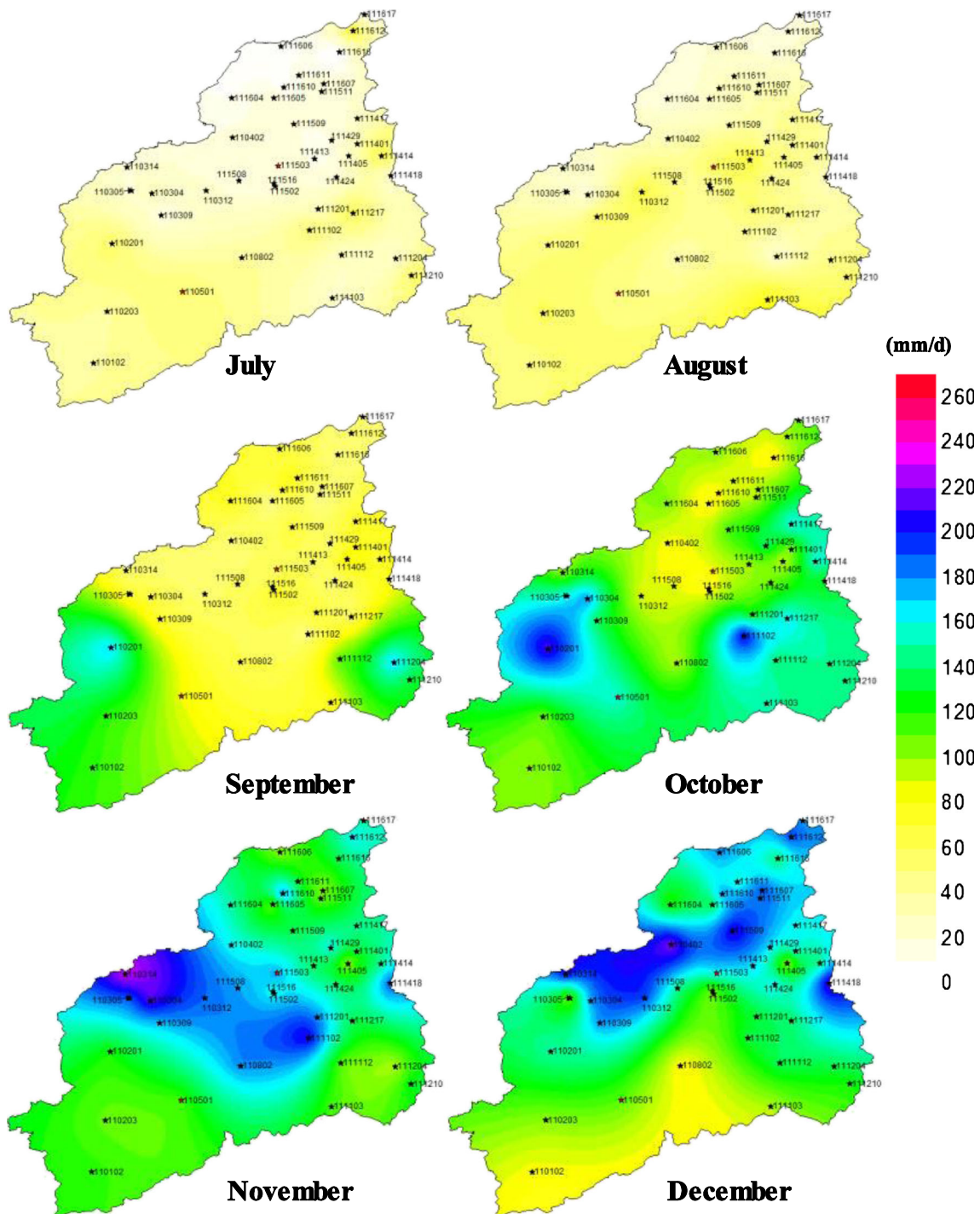


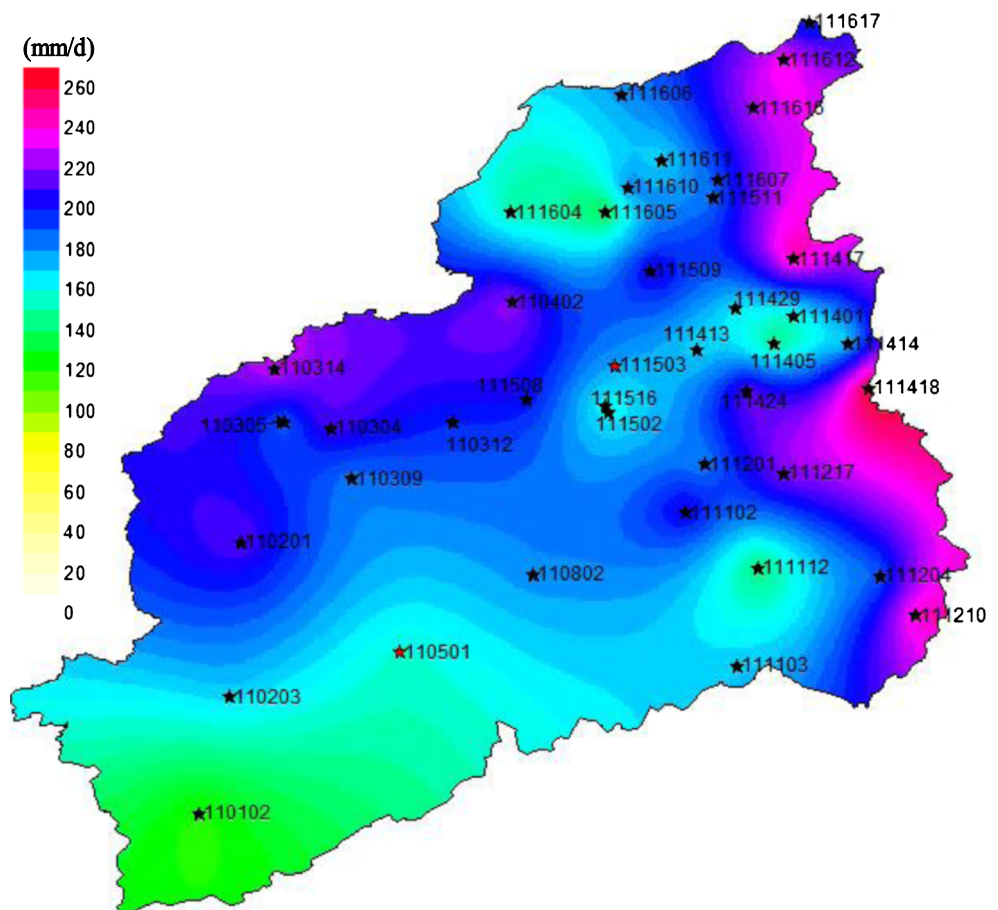
Fig. 5 (continued)

(r) and the regression slope (a). The correlation coefficient r is between -1 and $+1$ (Armatte 2001). The linear correlation coefficient between two characters X and Y (denoted r) is calculated by means of Eq. (2).

$$r = \frac{COV(x,y)}{\sigma_x \sigma_y} \tag{2}$$

- If r tends to 1 , there is a strong positive linear correlation between x and y .
- If r tends to 0 , there is no linear correlation between x and y ; they are independent.
- If r tends to -1 , there is a strong negative linear correlation between x and y .

Fig. 7 Maximum annual rainfall



precipitation at a fine spatial scale (Laborde 1984; Weisse 1998). Mapping makes it possible to evaluate the spatial variability of possible future results from descriptive statistics (Berthelot 2008). It is also possible to specialize punctual information.

The geostatistical approach (Kriging) was adopted after identifying the space structure based on the values measured in the stations (Hevesi et al. 1992).

Kriging is a stochastic method of spatial interpolation that estimate the value (s) of the regionalized variable under study sampled by a combination of data at the point measures while taking into account the distance and degree of variation between them (Baillargeon 2005). It is a linear unbiased estimation method and minimizes the estimation variance (Lawin et al. 2012).

It was used in this study the ordinary Kriging which is the more frequently used (Gratton 2002).

The first step is to build the experimental variogram and estimate its model. The second step is to use the model variogram for determine the weights of the samples that will be used for Kriging.

(a) Monthly maxima maps

Figure 5 shows the maps of daily rainfall maxima for the 12 months:

- The months January and February are characterized by a homogeneous distribution of extreme rainfall over the whole basin, which varies between 40 and 150 mm/day. Only a small area in the eastern part is marked by heavy rain, up to 230 mm/day.

- For the months March and April, the heaviest extreme rainfalls tilt towards the west of the basin (220 mm/day). The rest of the basin preserves the trend compared to previous months.

- The month of May has the same distribution as the two previous months except that the intensity of the rainfall is distinguished by its peak (263.7 mm/day at the station Nesmoth HF (111418) for the year 1970).

- The months of June, July, and August show a homogeneous distribution of low daily rainfall maxima ranging from 10 to 100 mm/day. Higher values (up to 160 mm/day) begin to appear in the south of the basin during the month of September.

- For the months of October, November, and December, extreme rainfall increases in intensity (100 mm/day to

Table 3 Trends in *r* values according to Westmacott

Category period	SIT	MIT	NST	MDT	SDT
I (<i>n</i> = 23)	$r > 0.351$	$0.277 < r \leq 0.351$	$-0.277 \leq r \leq 0.277$	$-0.351 < r \leq -0.277$	$r < -0.351$
II (<i>n</i> = 19)	$r > 0.388$	$0.307 < r \leq 0.388$	$-0.307 \leq r \leq 0.307$	$-0.388 < r \leq -0.307$	$r < -0.388$

240 mm/day) throughout the basin with high values in the center and north.

(b) Seasonal maxima maps

The following interpretations can be made as for the seasonal maxima series:

- In the summer, the daily rainfall maxima map (Fig. 6) shows a homogeneous distribution of rainfall ranging from 10 to 100 mm/day.

- The autumn season (Fig. 6) is characterized by an increasing trend of extreme values especially in the center of the basin (100 mm/day to 220 mm/day).
- In winter, the highest values move north and east with the same intensity of autumn (100 mm/day to 220 mm/day).
- In the spring, the highest values of extreme rainfall (263.7 mm/day) occur east of the watershed.

(c) Annual maxima map

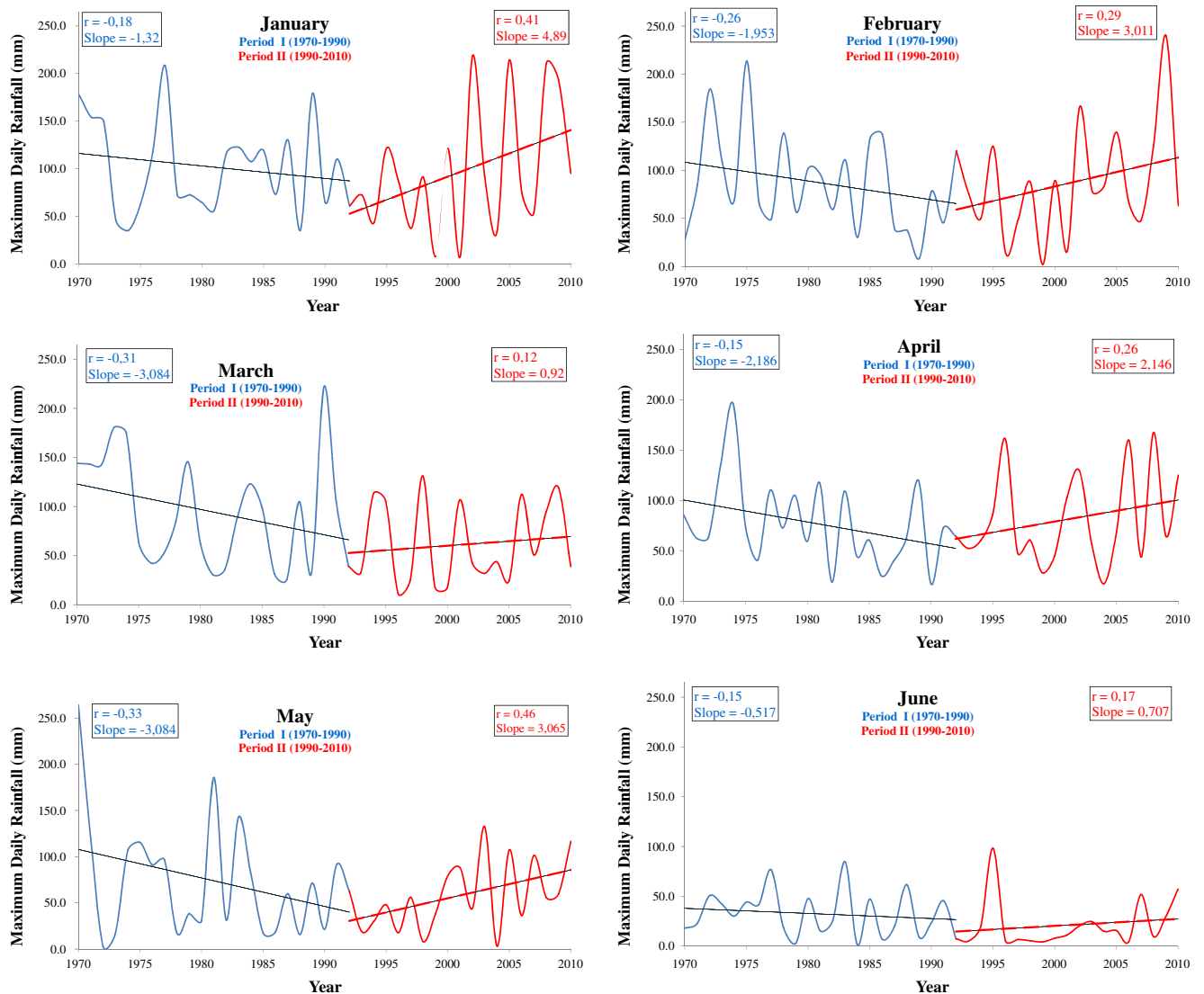


Fig. 8 Monthly maximum rainfall trends

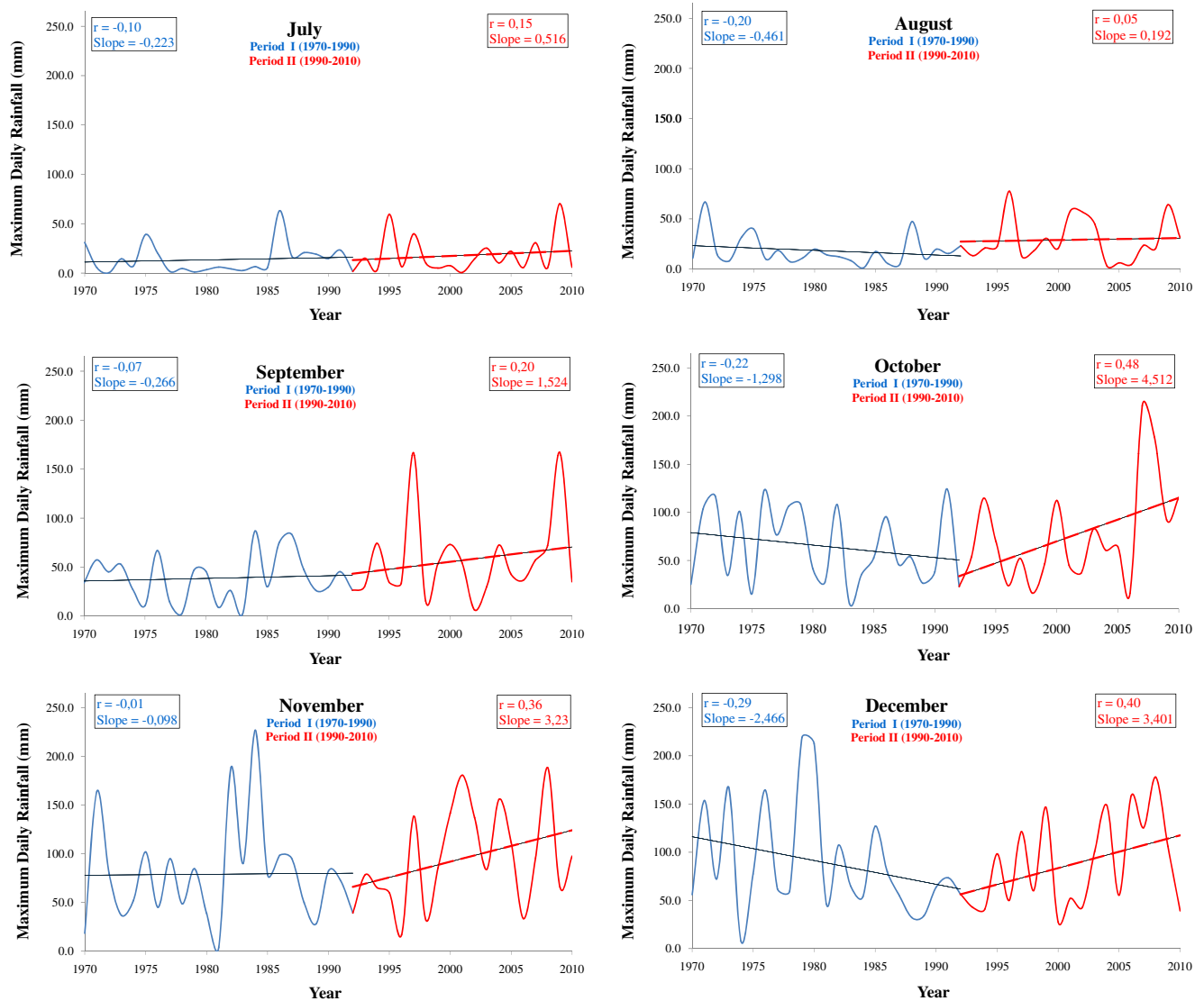


Fig. 8 (continued)

The values of daily extreme rainfall maxima fluctuate annually between 100 and 264 mm/day. The lowest rainfall of annual maxima occurs mainly in the south of the Macta Basin (Fig. 7) despite their geographical locations with maximum watershed altitudes. For example, the stations Ras El Ma (110102) and Ain El Hadjar (111103) with respective altitudes of 1105 m and 1097 m recorded daily maximum rainfall of magnitudes 100 mm/day to 160 mm/day. On the other hand, the highest rainfall of annual maxima is distributed in the North and East of the basin with minimum altitudes. For example, the station Marais de Sirat (111616), which is next to the Mediterranean Sea with only 30 m of altitude, records a maximum daily rain of 220 to 240 mm/day. The Nesmoth MF (111418) station at 930 m altitude recorded a maximum daily rainfall of 250 mm/day. Maximum daily rainfall values between 180 and 264 mm/day occupy 2/3 of the basin.

A linear regression was established between annual rainfall maxima and altitude, which resulted in an insignificant correlation.

Temporal variation of trends

The temporal analysis of the trends of the daily rainfall maxima of the Macta watershed over two periods (1970–1992 and 1992–2010) was carried out on a monthly, seasonal, and annual scale. Table 3 presents the trend categories according to the values of r , the series size n , and α value (Westmacott classification).

(a) Monthly trends

Table 4 Westmacott monthly trend classification using Pearson correlation coefficients (r) and regression line slopes (a)

Month	Period I (1970–1992)					Period II (1992–2010)				
	SIT	MIT	NST	MDT	SDT	SIT	MIT	NST	MDT	SDT
January			- 0,18 (- 1,32)			<i>0,41</i> (4,89)				
February			- 0,26 (- 1953)					0,29 (3011)		
March				- 0,31 (- 2582)				0,12 (0,920)		
April					- 0,36 (- 2186)			0,26 (2146)		
May					- 0,33 (- 3084)	<i>0,46</i> (3065)				
June		- 0,15 (- 0,517)						0,17 (0,707)		
July		0,10 (0,223)						0,15 (0,516)		
August		- 0,20 (- 0,461)						0,05 (0,192)		
September		0,07 (0,266)						0,20 (1524)		
October		- 0,22 (- 1298)				<i>0,48</i> (4512)				
November		0,01 (0,098)					<i>0,36</i> (3230)			
December					- 0,29 (- 2466)	<i>0,40</i> (3401)				

Table 4 contains the values of the Pearson correlation coefficients r and in parentheses are the values of the slopes (a) of each month. The values in italics are significant

The methodological approach cited above was applied in our Macta watershed study on extreme monthly, seasonal, and annual precipitation. Two graphical adjustments are obtained for the two periods I (in blue) and II (in red) with correlation coefficients (r) and slopes of the adjustment lines (a) as shown in Fig. 8.

The results obtained for the monthly maximum daily precipitation trends are shown in Table 4.

The comparison between the two periods I and II allows to deduce that the 7 months of February, March, April, June, July, August, and September do not show

perceptible changes. Climate change has affected exclusively the months of January, May, October, November, and December.

The remaining 5-month trends have shifted from non-trend or moderate decline (period I) to strong or moderate growth (period II).

(b) Seasonal trends

Figure 9 presents the trends of daily extreme rainfall maxima recorded during the four seasons of the year.

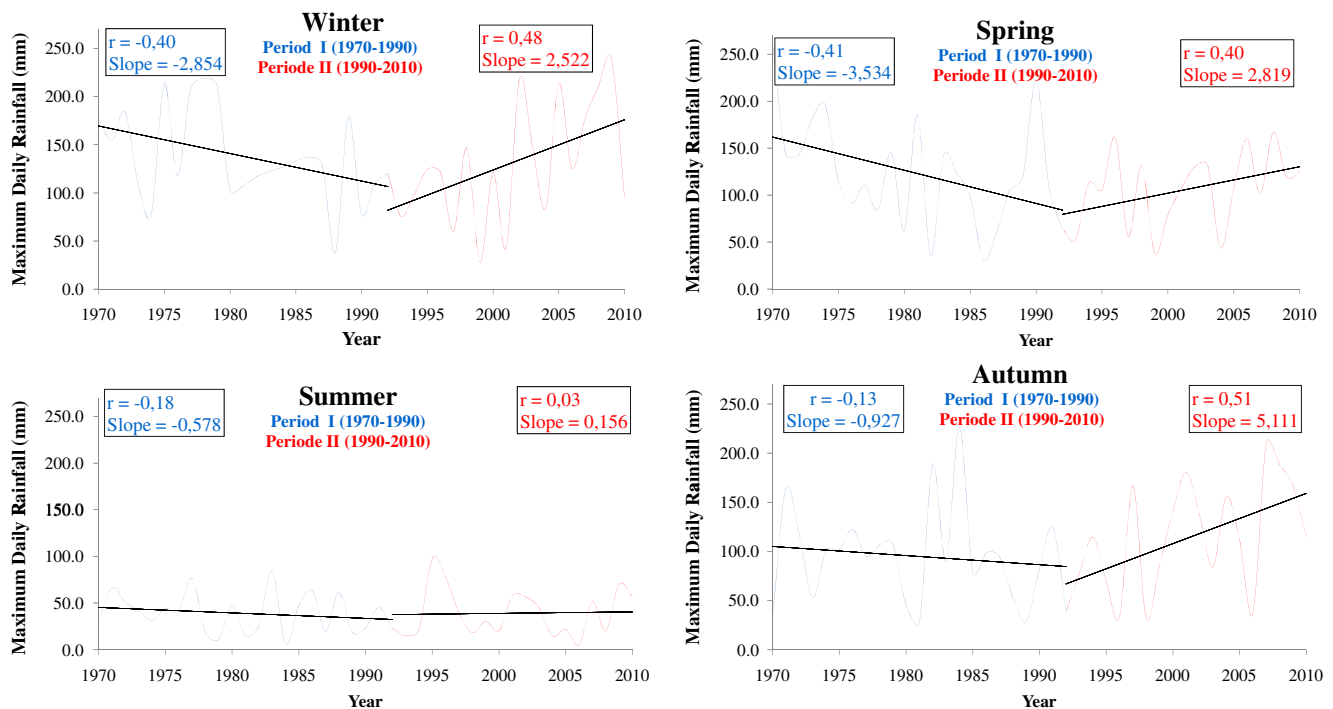


Fig. 9 Seasonal maximum rainfall trends

Table 5 Westmacott seasonal trends classification using Pearson correlation coefficients (*r*) and regression lines slopes (*a*)

Saison	Period I (1970–1992)					Period II (1992–2010)				
	SIT	MIT	NST	MDT	SDT	SIT	MIT	NST	MDT	SDT
Winter					<i>- 0,40 (- 2854)</i>	<i>0,48 (5221)</i>				
Spring					<i>- 0,41 (- 3534)</i>	<i>0,40 (2819)</i>				
Summer			- 0,18 (- 0,578)					0,03 (- 0,156)		
Autumn			- 0,13 (- 0,927)			<i>0,51 (5111)</i>				

Table 5 contains the values of the Pearson correlation coefficients *r* and in parentheses are the values of the slopes (*a*) of each season. The values in italics are significant

The winter and spring seasons (Table 5) have shifted from the sharp decline (period I) to the high growth (period II). Autumn switches from non-trend (period I in blue) to strong growth (period II in red). Summer maintains the no trend case both periods. In general, 3/4 or (75%) of seasons are affected by climate change.

(c) Annual trend

The analysis of the annual trend of maximum daily rainfall is shown in Fig. 10.

Climate change appears clearly as in Table 6, where the shift from the sharp decline (period I) to the high growth (period II) has been noted.

Spatial variation of trends

The same scientific approach was applied in space on 41 rainfall stations in the Macta watershed for maximum annual rainfall extremes. The results are presented in Table 7.

Figure 11 shows the spatial variation in annual maximum precipitation trends for the 41 stations during the two periods:

1. Period I (1970–1992): Here, 14 stations have a strongly decreasing trend (SDT) and 4 stations have a moderate decreasing trend (MDT) (Table 7). About 44% of the stations have decreasing trends in the north and east of the basin (Fig. 11a). On the other hand, 23 stations (56%) show no significant trend (NST) and are located in the center and south parts of the study area.

Fig. 10 Maximum annual rainfall trend

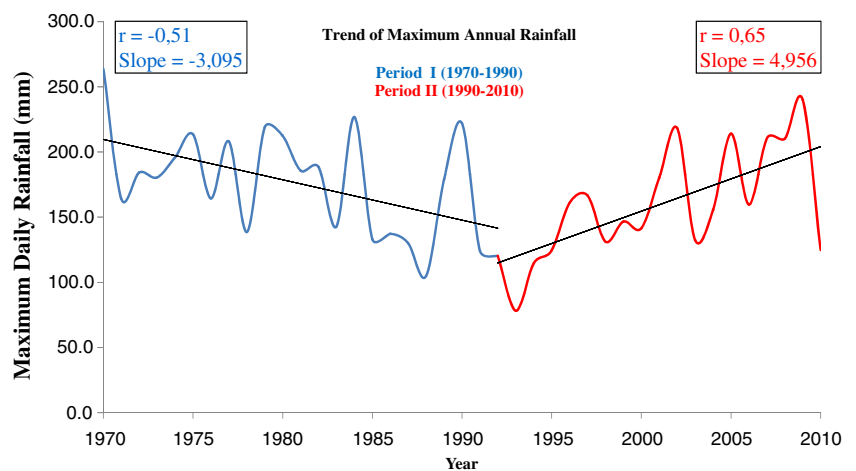


Table 6 Westmacott annual trend classification using Pearson correlation coefficients (*r*) and regression line slopes (*a*)

Year	Period I (1970–1992)					Period II (1992–2010)				
	SIT	MIT	NST	MDT	SDT	SIT	MIT	NST	MDT	SDT
<i>r</i> annual					<i>- 0,51 (- 3095)</i>	<i>0,65 (- 4956)</i>				

Table 4 contains the values of the Pearson correlation coefficients *r* and in parentheses are the values of the slopes (*a*). The values in italics are significant

Table 7 Westmacott classification using Pearson correlation coefficients and slope of regression lines of 41 stations

Station name	Code station	Period I (1970–1992)		Period II (1992–2010)	
		Coefficient de Pearson (<i>r</i>)	Slope (<i>a</i>)	Coefficient de Pearson (<i>r</i>)	Slope (<i>a</i>)
RAS EL MA	110,102	-0,13 ^{NST}	-0,395	0,51 ^{SIT}	2487
SID ALI BEN YOUB	110,201	-0,04 ^{NST}	-0,244	0,33 ^{MIT}	2478
EL HACAIBA	110,203	-0,24 ^{NST}	-1182	0,52 ^{SIT}	2306
SARNO Bge	110,304	-0,24 ^{NST}	-1596	0,36 ^{MIT}	2119
SIDI BEL ABBES	110,305	-0,11 ^{NST}	-0,577	0,43 ^{SIT}	1940
HASSI DAHO	110,309	-0,24 ^{NST}	-1277	0,55 ^{SIT}	3282
MOSTEFA BEN BRAHIM	110,312	-0,15 ^{NST}	-0,087	0,06 ^{NST}	0,293
AIN TRID	110,314	-0,11 ^{NST}	-0,702	0,28 ^{NST}	1559
CHEURFAS BGE	110,402	-0,23 ^{NST}	-1670	0,14 ^{NST}	0,683
MERINE	110,501	-0,15 ^{NST}	-0,660	0,56 ^{SIT}	2725
DAOUD YOUB	110,802	0,17 ^{NST}	-0,858	0,23 ^{NST}	0,074
MEFTAH SIDI BOUBEKEUR	111,102	-0,20 ^{NST}	-1084	0,41 ^{SIT}	2756
AIN EL HADJAR	111,103	-0,18 ^{NST}	-0,986	0,35 ^{MIT}	1527
HAMMAM RABI	111,112	-0,28 ^{MDT}	-1279	0,55 ^{SIT}	2415
OUED TARIA	111,201	-0,38 ^{SDT}	-2247	0,41 ^{SIT}	1242
AIN TIFRIT	111,204	-0,24 ^{NST}	-1160	0,42 ^{SIT}	2710
TAMESNA	111,210	-0,06 ^{NST}	-0,252	0,52 ^{SIT}	4274
BENIANE	111,217	-0,18 ^{NST}	-0,849	0,47 ^{SIT}	3701
MAOUSSA	111,401	-0,39 ^{SDT}	-1548	0,44 ^{SIT}	1722
MATEMORE	111,405	-0,38 ^{SDT}	-1250	0,16 ^{NST}	0,467
TIZI	111,413	-0,22 ^{NST}	-0,989	0,43 ^{SIT}	1584
SIDI KADA	111,414	-0,41 ^{SDT}	-1772	0,66 ^{SIT}	3817
AIN FARES	111,417	-0,28 ^{MDT}	-1590	0,43 ^{SIT}	2893
NESMOTH MF	111,418	-0,55 ^{SDT}	-4087	0,56 ^{SIT}	5,03
GHRISS	111,424	-0,60 ^{SDT}	-4033	0,24 ^{NST}	0,677
MASCARA	111,429	-0,25 ^{NST}	-1295	0,58 ^{SIT}	3044
SAHOUET OUIZERT	111,502	-0,14 ^{NST}	-0,605	0,20 ^{NST}	0,620
BOU HANIFIA BGE	111,503	-0,12 ^{NST}	-0,631	0,15 ^{NST}	0,467
SFISSEF	111,508	-0,18 ^{NST}	-1091	0,28 ^{NST}	1388
HACINE	111,509	-0,28 ^{MDT}	-1816	0,27 ^{NST}	1216
MOHAMMADIA GRHA	111,511	-0,47 ^{SDT}	-2753	0,37 ^{MIT}	1772
TROIS RIVIERES	111,516	-0,47 ^{SDT}	-2711	0,28 ^{NST}	0,626
OGGAZ	111,604	-0,40 ^{SDT}	-1720	0,25 ^{NST}	1196
BOU HENNI	111,605	-0,49 ^{SDT}	-1981	0,28 ^{NST}	1006
FORNEKA	111,606	-0,42 ^{SDT}	-2379	0,34 ^{MIT}	1557
SAMOURIA	111,607	-0,31 ^{MDT}	-1472	0,10 ^{NST}	0,349
MOCTA DOUZ	111,610	-0,23 ^{NST}	-1042	0,56 ^{SIT}	4318
FERME BLANCHE	111,611	-0,50 ^{SDT}	-2594	0,31 ^{MIT}	1389
BLED TAOURIA	111,612	-0,41 ^{SDT}	-2722	0,44 ^{SIT}	2637
MARAIS DE SIRAT	111,616	-0,58 ^{SDT}	-3536	0,45 ^{SIT}	2326
FERME ASSORAIN	111,617	-0,18 ^{NST}	-0,961	-0,15 ^{NST}	-0,689

SDT strong decreasing trend, *MDT* moderate decreasing trend, *NST* no significant trend, *MIT* moderate increasing trend, *SIT* strong increasing trend
 The values in italics are significant

2. Period II (1992–2010): This period is characterized by a totally opposite situation to the first, that is to say that the

significant upward trend appears in 26 stations (63%), divided between moderate (MIT) and strong (SIT) (see

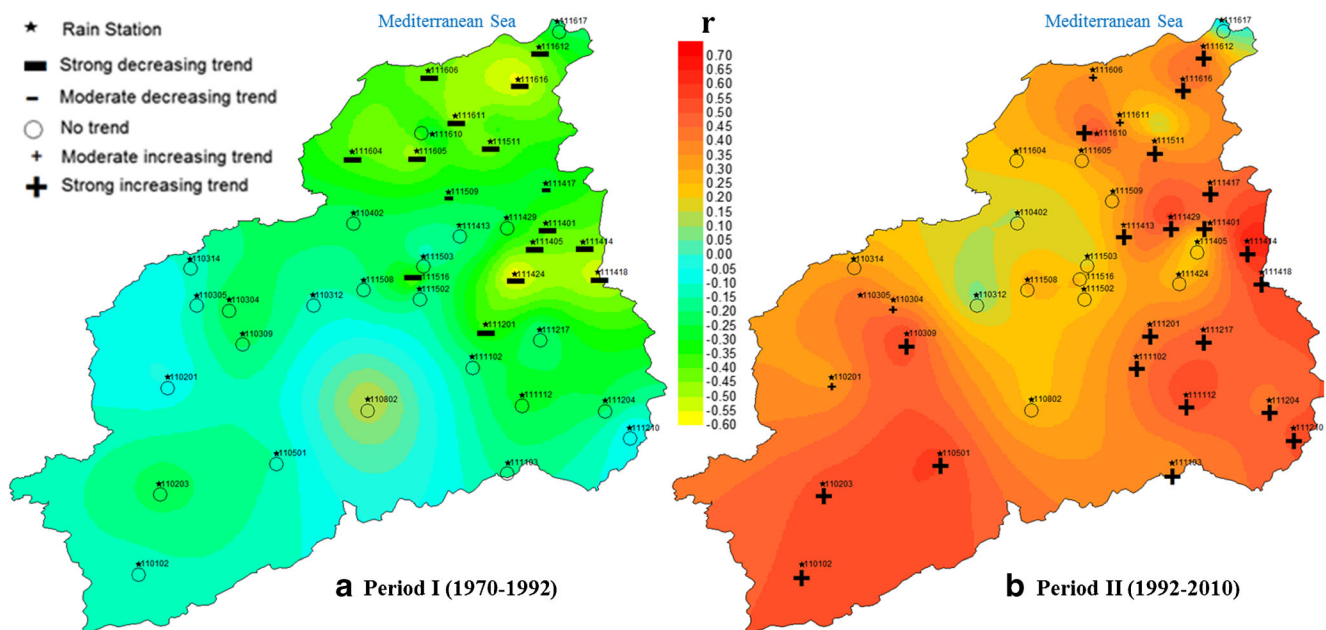


Fig. 11 Maximum annual daily precipitation trends for Macta stations. The color scale shows the coefficients of Bravais-Pearson r . The symbols show the sign of the precipitation trend of the 41 stations

Fig. 11b). The growing stations are distributed over all regions of the basin. About 37% of the stations show no significant trend (NST) and they are in the center of the basin.

In Fig. 11, we find that Pearson's correlation coefficients r move upward from the first to the second period. This situation is in perfect agreement with Fig. 7, which presents the distribution of the annual maxima of daily extreme rainfall. This implies the predominance of the trends of the second period on the first one.

The results of this study detect significantly increasing trends in extreme monthly, seasonal, and annual precipitation. Paradoxically, Elouissi et al. (2016) detected a decreasing trend of total precipitation in the same watershed during the period 1970–2011.

These results converge with the work of several authors (Caloiero et al. 2016; Brugnara et al. 2012; Alpert et al. 2002; Brunetti et al. 2001), who detected a paradoxical increase in the extreme precipitation records, despite a decrease in totals, in different areas of the Mediterranean basin.

Faced with different behavior of the extreme rains in the Mediterranean basin, we reiterate the suggestion of Reiser and Kutiel (2011) who propose a detailed regional analysis.

Conclusion

The purpose of this study is to analyze the time series of daily maximum precipitation, to map and to detect significant

trends. The study was conducted in the Macta watershed, and the following points are significant for consideration in any future project in the study area.

- The spatiotemporal distribution of daily extreme rainfall maxima releases values ranging from 118.3 to 264 mm/day. Their locations in the basin switch from 1 month to the next. The most extreme season is spring with 263.7 mm/day rainfall. The most extreme values are located in the North and East of the basin. The coefficients of variation vary between 27 and 48%.
- Among all years, 1992 was detected as a break-up date with the shift in monthly, seasonal, and annual trends from decline to significant growth.
- The first period (1970–1992) is characterized by a significant decrease in the trend in the months of March, April, May, and December. The winter and spring seasons show significantly decreasing trend. Annually, 18 stations (44%) have significantly decreasing trends and they are located in the North and East of the basin. On the other hand, 23 stations (56%) have no significant trend. None of the stations has shown a growing trend.
- The second period (1992–2010) shows a situation opposite to the first one. It implies significant growth in 5 months (January, May, October, November, and December) trends and three seasons (winter, spring, and autumn). It is obvious that the climate change affects all regions except the center of the basin. Annually, 63% of the stations have significantly increasing trends in the north, east, and even south of the watershed.

Acknowledgments The authors thank the National Water Resources Agency (ANRH) for the availability of data. The authors thank Professor Zohair Chentouf (King Saud University (KSA)) for his linguistic advice.

References

- Ague AI, Afouda A (2015) Analyse fréquentielle et nouvelle cartographie des maxima annuels de pluies journalières au Bénin. *Int J Biol Chem Sci* 9(1):121–133
- Alentorn A, Markose S (2005) Generalized extreme value distribution and extreme economic value at risk (EE-VaR)
- Alpert P, Ben-gai T, Baharad A, Benjamini Y, Yekutieli D, Colacino M, Diodato L, Ramis C, Homar V, Romero R, Michaelides S, Manes A (2002) The paradoxical increase of Mediterranean extreme daily rainfall in spite of decrease in total values. *Geophys Res Lett*, 29, 31–1–31–4. <https://doi.org/10.1029/2001GL013554>
- Armatte M (2001) The changing status of the correlation in econometrics (1910–1944). *Economic Review Flight* 52(3):617–631
- Baillargeon S (2005) Le krigeage: revue de la théorie et application à l'interpolation spatiale de données de précipitations. Mémoire de Maitrise, Université Laval, Québec 2005
- Bekoussa BS, Meddi M, Jourde H (2008) Forçage climatique et anthropique sur la ressource en eau souterraine d'une région semi-aride : cas de la plaine de Ghriss (Nord-Ouest algérien). *Sécheresse* 19(3):173–184
- Bellu A, Sanches Fernandes LF, Cortes RMV, Pacheco FAL (2016) A framework model for the dimensioning and allocation of a detention basin system: the case of a flood-prone mountainous watershed. *J Hydrol* 533:567–580
- Berolo W, and Laborde JP (2003) Statistiques des précipitations journalières extrêmes sur les Alpes-Maritimes. Université Sophia Antipolis. Notice explicative de la carte au 1/200 000 et de ses annexes
- Berthelot A (2008) Diffusion spectrale et rétrécissement par le mouvement dans les boîtes quantiques. Thèse de Doctorat. Université Paris VI, Paris
- Blanchet J, Molinié G, Touati J (2018) Spatial analysis of trend in extreme daily rainfall in southern France. *Clim Dyn* 51:799–812. <https://doi.org/10.1007/s00382-016-3122-7>
- Brugnara Y, Brunetti M, Maugeri M, Nanni T, Simolo C (2012) High-resolution analysis of daily precipitation trends in the Central Alps over the last century. *Int J Climatol* 32:1406–1422
- Brunetti M, Maugeri M, Montif F, Nanni T (2001) Changes in total precipitation, rainy day and extreme events in Northeast Italy. *Int J Climatol* 861–871(2001):21
- Brunetti M, Maugeri M, Montif F, Nanni T (2005) Temperature and precipitation variability in Italy in the last two centuries from homogenized instrumental time series. *Int J Climatol* 345–381(2006):26
- Caloieroa T, Coscarelli R, Ferrari E, Sirangelo B (2016) Trends in the daily precipitation categories of Calabria (southern Italy). *Procedia Engineering* 162(2016):32–38
- Carvalho JRP, Assad ED, Oliveira AF, Pinto HS (2014) Annual maximum daily rainfall trends in the Midwest, southeast and southern Brazil in the last 71 years. *Weather and Climate Extremes* 5(6):7–15. <https://doi.org/10.1016/j.wace.2014.10.001>
- CCSP (2008) Weather and climate extremes in a changing climate, regions of focus: North America, Hawaii, Caribbean, and U.S. Pacific Islands. A report by the U.S. climate change science program and the subcommittee on global change research., [Thomas R. Karl, Gerald A. Meehl, Christopher D. Miller, Susan J. Hassol, Anne M. Waple and William L. Murray (eds.)]
- Cetin M, Kalayci Onac A, Sevik H, Canturk U, Akpinar H (2018a) Chronicles and geohéritage of the ancient Roman city of Pompeiopolis: a landscape plan. *Arab J Geosci* 11:798. <https://doi.org/10.1007/s12517-018-4170-6>
- Cetin M, Zeren I, Sevik H, Cakir C, Akpinar H (2018b) A study on the determination of the natural park's sustainable tourism potential. *Environ Monit Assess* 190:167. <https://doi.org/10.1007/s10661-018-6534-5>
- Chaouche K, Hubert P, Lang G (2002) Graphical characterisation of probability distribution tails. *Stoch Env Res Risk A* 16(5):342–357. <https://doi.org/10.1007/s00477-002-0111-7>
- Deng S, Chen T, Yang N, Qu L, Li M, Chen D (2018) Spatial and temporal distribution of rainfall and drought characteristics across the Pearl River basin. *Sci Total Environ* 619–620:28–41
- Djedjai H (1997) State of the surface water quality of the Macta watershed. Algerian-French Cooperation Project, 1997 - Vol December 1997
- Donat et al (2014) Changes in extreme temperature and precipitation in the Arab region: long-term trends and variability related to ENSO and NAO. *Int J Climatol*
- Elouissi A, Şen Z, Habi M (2016) Algerian rainfall innovative trend analysis and its implications to Macta watershed. *Arab J Geosci* 9: 303. <https://doi.org/10.1007/s12517-016-2325-x>
- Elouissi A, Habi M, Benaricha B, Boualem SA (2017) Climate change impact on rainfall spatio-temporal variability (Macta watershed case, Algeria). *Arab J Geosci* 10:496. <https://doi.org/10.1007/s12517-017-3264-x>
- Goula BTA, Konan B, Brou YT, Savane I, Fadika V, Srohourou B (2007) Estimation des pluies exceptionnelles journalières en zone tropicale : cas de la Côte d'Ivoire par comparaison des lois lognormale et de Gumbel. *Journal des Sciences Hydrologiques* 52(2):49–67
- Gratton Y (2002) Le Krigeage : la méthode optimale d'interpolation spatiale. Les articles de l'Institut d'Analyse Géographique, www.iag.asso.fr
- Groisman PY, Knight RW, Easterling DR, Karl TR, Hegerl GC, Razuvaev VN (2005) Trends in intense precipitation in the climate record. *J Clim* 18:1326–1350
- Helsel DR, Hirsch MR (1993) *Statistical methods in water resources*. Elsevier Science 49 Publishers B.V
- Henderson KG, Muller RA (1997) Extreme temperature days in the south-Central United States. *Clim Res* 8:151–162
- Hevesi JA, Flint AL, Istok JD (1992) Precipitation estimation in mountainous terrain using multivariate Geostatistics. Part II: Isoyetal maps. *J Appl Meteorol* 31:677–688
- IPCC (Intergovernmental panel on climate change) (2007) The physical science basis, contribution of working group I to the fourth assessment report of the intergovernmental panel on climate change. Cambridge University Press, 2007
- IPCC (Intergovernmental Panel on Climate Change) (2013) Edited by Thomas F. Stocker Dahe Qin, Gian-Kasper Plattner Melinda M.B. Tignor Simon K. Allen Judith Boschung, Alexander Nauels Yu Xia Vincent Bex Pauline M. Midgley And working group I technical support unit, working group I contribution to the fifth assessment report of the intergovernmental panel on climate change (IPCC), summary for policymakers.
- Jenkinson AF (1955) The frequency distribution of the annual maximum (or minimum) values of meteorological elements'. *JQR Meteorol Soc* 81:145–158
- Keggenhoff I, Elizbarashvili M, Amiri-Farahani A, King L (2014) Trends in daily temperature and precipitation extremes over Georgia, 1971–2010. *Weather and Climate Extremes* 4(2014):75–85
- Kioutsoukis I, Melas D, Zerefos C (2010) Statistical assessment of changes in climate extremes over Greece (1955–2002). *Int J Climatol* 30:1723–1737

- Klein Tank AMG, Können GP (2003) Trends in indices of daily temperature and precipitation extremes in Europe, 1946–99. *J Clim* 16: 3668–3680
- Kostopoulou E, Jones PD (2005) Assessment of climate extremes in the eastern Mediterranean. *Meteorog Atmos Phys* 89:69–85
- Koutsoyiannis D (2004) Statistics of extremes and estimation of extreme rainfall: II. Empirical investigation of long rainfall records. *Hydrological Sciences–Journal–des Sciences Hydrologiques*, 49(4) August 2004
- Laborde JP (1984) Analyse des données et cartographie automatique en hydrologie : éléments d'hydrologie Lorraine. Thèse de Doctorat d'Etat, INPL, Nancy, 484 p
- Lawin EA, Oguntunde PG, Lebel T, Afouda A, Gosset M (2012) Rainfall variability at regional and local scales in the Ouémé Upper Valley in European scientific journal April 2014 edition vol.10, No.11 ISSN: 1857–7881 (print) e - ISSN 1857–7431 274
- Longobardi A, Villani P (2009) Trend analysis of annual and seasonal rainfall time series in the Mediterranean area. *International Journal of Climatology Int J Climatol*, n/a
- Lopez-Moreno JI, Vicente-Serrano SM, Moran-Tejeda E, Zabalza J, Lorenzo-Lacruz J, Garcia-Ruiz JM (2011) Impact of climate evolution and land use changes on water yield in the Ebro basin. *Hydrol Earth Syst Sci* 15:311–322
- Mannshardt-Shamseldin EC, Smith RL, Sain SR, Mearns LO, Cooley D (2010) Downscaling extremes: a comparison of extreme value distribution in point-source and gridded precipitation data. *Ann Appl Stat* 4(1):484–502
- Martinez MD, Lana X, Burguenoc A, Serra C (2007) Spatial and temporal daily rainfall regime in Catalonia (NE-Spain) derived from four precipitation indices, years 1950–2000. *Int J Climatol* 27:123–138
- Meddi H, Assani A (2014) Study of drought in seven Algerian Plains. *Arab J Sci Eng* 39(1):339–359
- Meddi M, and Hubert P (2003) Impact de la modification du régime pluviométrique sur les ressources en eau du Nord-Ouest de l'Algérie. *Hydrology of the Mediterranean and semi arid Regions*. IAHS publication N° 278
- Meddi M, Toumi S (2013) Study of the interannual rainfall variability in northern Algeria. *Rev Sci Tech LJEE* N°23. Décembre 2013
- Meddi M, Talia A and Martin C (2009) Évolution récente des conditions climatiques et des écoulements sur le bassin versant de la Macta (Nord-Ouest de l'Algérie). *Physio-Géo* [Online], Volume 3. <http://physio-geo.revues.org/686#entries>
- Min SK, Zhang X, Zwiers FW, Hegeri GC (2011) Human contribution to more-intense precipitation extremes. *Nature* 470:2011
- Muller A (2006) Comportement de la distribution asymptotique des pluies extrêmes en France. Thèse de l'Université de Montpellier II, 182 p
- Onibon H, Ourda TBM, Barbet M, St-Hilaire A, Bobee B and Bruneau P (2004) Analyse fréquentielle régionale des précipitations journalières maximales annuelles au Québec, Canada. *Hydrological Sciences–Journal–des Sciences Hydrologiques*, 49 (4) août
- Onyutha C (2015) Identification of sub-trends from hydro-meteorological series. *Stoch Env Res Risk A* 30:189–205. <https://doi.org/10.1007/s00477-015-1070-0>. in press
- Pandey KC (2014) Extreme point rainfall events analysis of Gorakhpur under climate change scenario. *Journal of Climatology & Weather Forecasting* 2(1). <https://doi.org/10.4172/2332-2594.1000107>
- Parry M, Rosenzweig CA, Iglesias M, Livermore M, Fisher G (2004) Effects of climate change on global food production under SRES emissions and socioeconomic scenarios. *Glob Environ Chang* 14(1): 53–67
- Reiser H, Kutiel H (2011) Rainfall uncertainty in the Mediterranean: time series, uncertainty, and extremes. *Theor Appl Climatol* 104(2010): 357–375
- Şen Z (2012) Innovative trend analysis methodology. *J Hydrol Eng* 17(9): 1042–1046
- Shang H, Yan J, Gebremichael M, Ayalew M (2011) Trend analysis of extreme precipitation in the northwestern highlands of Ethiopia with a case study of Debre Markos. *Hydrol Earth Syst Sci* 15:1937–1944
- Sharad KJ, Kumar V (2012) Trend analysis of rainfall and temperature data for India. *Curr Sci* 102(1):37–49. 10 January 2012
- Sharad KJ, Nayak PC, Singh Y and Chandniha SK (2017) Trends in rainfall and peak flows for some river basins in India. *Curr Sci*, Vol. 112, NO. 8, 25 APRIL 2017
- Subak S, Palutikof JP, Agnew MD, Watson SJ, Bentham CG, Cannell MGR, Hulme M, McNally S, Thornes JE, Waughray D, Woods JC (2000) The impact of the anomalous weather of 1995 on the U.K. economy. *Clim Chang* 44:1–26
- Terêncio DPS, Sanches Fernandes LF, Cortes RMV, Pacheco FAL (2017) Improved framework model to allocate optimal rainwater harvesting sites in small watersheds for agro-forestry uses. *J Hydrol* 550:318–330
- Terêncio DPS, Sanches Fernandes LF, Cortes RMV, Moura JP, Pacheco FAL (2018) Rainwater harvesting in catchments for agro-forestry uses: a study focused on the balance between sustainability values and storage capacity. *Sci Total Environ* 613-614:1079–1092
- Tramblay Y, El Adlouni S, Servat E (2013) Trends and variability in extreme precipitation indices over Maghreb countries. *Nat Hazards Earth Syst Sci* 13:3235–3248
- Weisse KA (1998) Etude des précipitations exceptionnelles de pas de temps court en relief accidenté (Alpes françaises) - Méthode de cartographie des précipitations extrêmes. Thèse de Doctorat, LTHE - INPG, Grenoble, 314 p
- Westmacott JR, Burn DH (1997) Climate change effects on the hydrologic regime within the Churchill-Nelson River basin. *J Hydrol* 202: 263–279
- Westra S, Alexander LV, Zwiers FW (2012) Global increasing trends in annual maximum daily precipitation. 3904 *Journal of climate* Volume 26
- Wilks DS, Cember RP (1993) Atlas of precipitation extremes for the northeastern United States and southeastern Canada. Northeast Regional Climate Center Research Series
- Zalina MD, Desa MN, Nguyen V-T-V, Kassim AH (2002) Selecting a probability distribution for extreme rainfall series en Malaysia. *Water Sci Technol* 45:63–68